J. Fluid Mech. (1977), vol. 83, part 1, pp. 177–190
Printed in Great Britain

Variable-viscosity flows in heated and cooled channels

By H. OCKENDON
Somerville College, Oxford

AND J. R. OCKENDON
Computing Laboratory, 19 Parks Road, Oxford

(Received 4 January 1977 and in revised form 20 May 1977)

An asymptotic description is given of Newtonian fluid flow in a channel which is suddenly heated or cooled. The viscosity is assumed to be purely a function of temperature. The asymptotic approximation is that the downstream viscosity at the channel wall differs by an order of magnitude from that in the upstream flow. Although we make the drastic assumption that viscous dissipation is negligible, we can analyse flows where the viscosity depends either algebraically or exponentially on the temperature.

1. Introduction

The aim of this paper is to provide a qualitative theoretical description of the effect of a sudden increase or decrease in the wall temperature on the flow of a Newtonian fluid in a narrow channel. Such a description is possible when the viscosity is either weakly or strongly dependent on temperature, and we shall analyse the latter situation here. Our motivation comes from the study of rheometers and injection-moulding devices, the realistic modelling of which usually requires a numerical solution. Our principal hope is that these results can be used as a check on computer models for real flows when viscosity variations are large enough to pose numerical difficulties and in particular we shall try to describe clearly the mechanical and thermal boundary layers which can then arise. In practice our solutions describe only high Prandtl number flows, say of oils, when in addition both the imposed temperature difference is large enough for the Brinkman number to be small, and smaller than the Nahme–Griffith number, and the channel width is small enough for the Péclet number to be large. The fact that the Prandtl number is large also ensures that the mechanical relaxation length along the channel is much less than the thermal relaxation length and we therefore assume a fully developed Poiseuille flow, with uniform temperature T_1, dynamic viscosity μ_1 and maximum speed $\frac{1}{2}U$ at the point $x = 0$ at which the wall temperature is changed. We also assume that the fluid has constant density ρ, constant specific heat c and, for mathematical convenience, constant thermal conductivity k. For most of this paper we shall discuss two-dimensional flow. The very similar analysis for the axisymmetric case will be described briefly in the appendix.

To be more precise, in two-dimensional flow we non-dimensionalize by writing the transverse co-ordinate as hy, where y is half the channel breadth; the downstream co-ordinate as Lx, where $L = \rho ch^2U/k$ is the length over which downstream convection balances transverse conduction; the velocity as $(Uu, hUv/L)$; the pressure as $\mu_1 UL/h^2$; the viscosity $\tilde{\mu}(\tilde{T})$ as $\mu_1\mu(T)$; and the temperature difference $\tilde{T}-T_1$ as $(\Delta T)T$, where ΔT is the imposed temperature difference. The Navier–Stokes equations become

$$u_x+v_y = 0, \tag{1.1}$$

$$O\left(\frac{k}{\mu_1 c}\right) = -p_x+(\mu u_y)_y+O\left(\frac{h^2}{L^2}\right), \tag{1.2}$$

$$O\left(\frac{h^2}{L^2}\frac{k}{\mu_1 c}\right) = -p_y+O\left(\frac{h^2}{L^2}\right), \tag{1.3}$$

$$uT_x+vT_y = T_{yy}+O\left(\frac{h^2}{L^2},\frac{\mu_1 U^2}{k\Delta T}\right), \tag{1.4}$$

with boundary conditions

$$v = T = 0, \quad u = \tfrac{1}{2}(1-y^2) \quad \text{at} \quad x = 0 \tag{1.5}$$

and

$$T\mp 1 = u = v = 0 \quad \text{at} \quad |y| = 1 \tag{1.6a,b}$$

in the heated and cooled cases respectively.

The assumption of large Prandtl number $\mu_1 c/k$ allows us to neglect the inertia terms in (1.2) and (1.3); that of large Péclet number L/h allows us to make the lubrication approximation; and that of small Brinkman number $\mu_1 U^2/k\Delta T$ allows us to neglect viscous dissipation in (1.4). Pearson (1977) discusses flows with rapidly varying viscosity where dissipation is entirely responsible for the temperature variations.

Introducing a stream function ψ, our dimensionless model becomes (with a prime denoting d/dx)

$$p_x = p'(x), \quad \mu(\beta T)\psi_{yy} = yp', \tag{1.7a,b}$$

$$\psi_y T_x-\psi_x T_y = T_{yy}, \tag{1.8}$$

with

$$T = 0, \quad \psi = -\tfrac{1}{6}y^3+\tfrac{1}{2}y \quad \text{at} \quad x = 0 \tag{1.9}$$

and

$$T\mp 1 = \psi_x = \psi_y = 0 \quad \text{at} \quad |y| = 1, \tag{1.10}$$

where $-p'(0) = \mu(0) = 1$. The dimensionless parameter β is the ratio of the Nahme–Griffith number $U^2k^{-1}d\tilde{\mu}/d\tilde{T}$ to the Brinkman number and measures the sensitivity of the viscosity to changes in temperature. Our asymptotic approximation will be that $\beta \gg 1$ and $\mu(-\beta) \gg 1 \gg \mu(\beta)$. We shall find that this approximation predicts flows in which there are rapid changes in both the scaled x and the scaled y direction. If, in a real situation, the rapidity of these changes invalidates our original choice of length scales, we hope our solution will still be of value as a limiting one against which to compare the numerous numerical solutions of (1.7)–(1.9) and their generalizations (see, for example, Hieber 1977, private communication; Horve 1974; Lord & Williams 1975).

In both the heated- and the cooled-wall problems, mass conservation ensures that the velocity returns to its original Poiseuille profile sufficiently far downstream, at a greatly reduced or increased pressure gradient respectively. There is no non-uniqueness about this steady state as there could be were dissipation important. However, this does not guarantee the stability of the flows we are about to describe. Indeed the jet-like flows which occur when the wall is cooled do suggest instability, but we shall consider only the steady-state problem here (see Lebon & Nguyen (1974) and Craik (1968) for a discussion of the stability of the fully developed flow).

Before we consider the detailed solution of (1.7)–(1.10) in various cases, we note that a boundary-layer analysis of these equations is always possible when x is sufficiently small for the pressure gradient to be still near -1, the velocity field away from the walls being close to (1.9). The temperature then differs appreciably from zero only in thermal boundary layers which, since (1.9) gives

$$\psi \sim -\tfrac{1}{3} + \tfrac{1}{2}(y+1)^2 \quad \text{as} \quad y \to -1, \tag{1.11}$$

are of thickness $O(x^{\frac{1}{3}})$. The boundary layers even admit a similarity solution of the form

$$\psi + \tfrac{1}{3} = x^{\frac{2}{3}} f(\zeta), \quad T = g(\zeta), \quad \text{where} \quad \zeta = (y+1)/x^{\frac{1}{3}}, \tag{1.12}$$

and

$$\mu(\beta g)\, d^2 f/d\zeta^2 = 1, \quad d^2 g/d\zeta^2 + \tfrac{2}{3} f\, dg/d\zeta = 0, \tag{1.13a,b}$$

with

$$g \mp 1 = f = df/d\zeta = 0 \quad \text{at} \quad \zeta = 0. \tag{1.14a,b}$$

For values of $\beta \leqslant O(1)$, these boundary layers grow and merge when x reaches $O(1)$, the flow finally reverting to isothermal Poiseuille flow as $x \to \infty$. For small β, an explicit description of the process can be given as a perturbation about the solution to the Graetz problem, $\beta = 0$ (Galili, Takserman-Krozer & Rigbi 1975). In fact, when $\beta = 0$ there is an eigenfunction expansion for the solution of (1.8) for any x but even then the explicit 'Leveque' solution of (1.13) and (1.14) is still helpful for $x \ll 1$ (Munahata 1975).

The next two sections of this paper will discuss the solution of (1.7)–(1.10) for large β in the cases of heated and cooled walls respectively. In both cases the entry solution (1.13) will still apply for sufficiently small x, depending now on β. The original motivation for some of the scalings came from the consideration of the simplified problem in which μ is a suitably centred and scaled step function of T. The flow then becomes a free-boundary problem consisting of two regions of constant viscosity and in situations for which there is a similarity solution this enabled us to solve the equations explicitly. This approach was particularly helpful for the cooled-wall problem, when it showed that the viscosity change occurred at an $O(1)$ distance from the wall, which suggested a solution for more general μ with a free-layer structure as described in §3.1.2.

2. Heated channel wall

2.1. *Algebraic viscosity*

We first consider the case where μ decreases algebraically as βT increases such that $\mu(\beta T)/\mu(\beta) = O(1)$ as $\beta \to \infty$ for $T = O(1)$. The case of exponential decrease is roughly similar and will be considered later.

2.1.1. *Entry region.* We begin by describing the solution of (1.13) for small values of $\mu(\beta) = \mu_0$, say. We note that $O(1)$ variations in g can occur only when both $f/\zeta^2 = O(1/\mu_0)$ and $f = O(1/\zeta)$, so we redefine

$$\zeta = \mu_0^{\frac{1}{3}} \zeta_1, \quad f = \mu_0^{-\frac{1}{3}} f_1 \tag{2.1}$$

n	0·5	1	2	5	10
a	1·75	1·20	0·799	0·445	0·277

TABLE 1. Values of the asymptotic constant a for different viscosities.

to give

$$\mu(\beta g)\frac{d^2f_1}{d\zeta_1^2} = \mu_0, \quad \frac{d^2g}{d\zeta_1^2}+\tfrac{2}{3}f_1\frac{dg}{d\zeta_1} = 0. \tag{2.2a, b}$$

Now this sublayer can have a chance of matching with the core Poiseuille flow only if

$$g \to 0 \quad \text{as} \quad \zeta_1 \to \infty \tag{2.3}$$

to lowest order in μ_0. Moreover, in the case when $\mu(\beta g) = 1/(1+\beta g)^n$, so that (2.2$a$) is $g^{-n}d^2f_1/d\zeta_1^2 = 1$ to lowest order, there are only a triply infinite number of solutions for g satisfying (2.3). We thus assume in general that (2.3) renders the solution of (2.2) with boundary conditions (1.14a) unique. Indeed, numerical integration from $\zeta_1 = 0$ to $\zeta_1 = 5$ confirms the existence, for any n, of a positive constant a such that $f \sim a\zeta_1$ and $g = O(\zeta_1^{-1}\exp(-\tfrac{1}{3}a\zeta_1^2))$ as $\zeta_1 \to \infty$ and typical values of a are given in table 1.

However, while the temperature g then matches with the core as $\zeta_1 \to \infty$, the stream function does not. The sublayer must be complemented by an outer region in which $\zeta = O(\mu_0^{-\frac{2}{3}})$, $f = O(\mu_0^{-\frac{4}{3}})$ and g is exponentially small, and where

$$f \sim \mu_0^{-\frac{4}{3}}\{\tfrac{1}{2}(\mu_0^{\frac{2}{3}}\zeta)^2 + a(\mu_0^{\frac{2}{3}}\zeta)\} \tag{2.4}$$

to lowest order.

If we now ask how far downstream this thermal boundary layer extends, we can note either that (2.4) indicates a perturbation to the $O(1)$ core stream function which is $O(x^{\frac{1}{3}}/\mu_0^{\frac{2}{3}})$ or that the region in which f adjusts to its core value is at a distance $O(x^{\frac{1}{3}}/\mu_0^{\frac{2}{3}})$ from the wall. Either observation suggests that the core velocity ceases to satisfy the no-slip condition when x reaches $O(\mu_0^2)$. Then the core stream function $\psi \sim -\tfrac{1}{3}+\tfrac{1}{3}(1+p')(y+1)$ as $y \to -1$, and p' is no longer near -1.

2.1.2. *Slipping core region.* We are led to consider a new thermal boundary layer in which $x = O(\mu_0^2)$, $y+1 = O(\mu_0)$, $\psi+\tfrac{1}{3} = O(\mu_0)$, $p' = O(1)$ and in which

$$\mu(\beta T)\Psi_{YY} = -\mu_0 p', \tag{2.5}$$

$$\Psi_Y T_x - \Psi_x T_Y = T_{YY} \tag{2.6}$$

to lowest order. To avoid proliferation of suffixes here and henceforth we have written capitals for ψ and y when they are used as boundary-layer variables (e.g. in (2.5), $y+1 = \mu_0 Y$, $\psi+\tfrac{1}{3} = \mu_0\Psi$). The usual wall boundary condition (1.10a) is applied and matching with the slipping core requires that

$$T = o(1), \quad \Psi \sim \tfrac{1}{3}(1+p')Y \quad \text{as} \quad Y \to \infty. \tag{2.7}$$

Despite the variation of p', (2.5)–(2.7) still admit a similarity solution

$$T = g(\xi), \quad \Psi = (\tfrac{2}{3})^{\frac{2}{3}}\frac{\lambda^2(1+p')^2}{(-p')}f_1(\xi), \quad \text{where} \quad \xi = -(\tfrac{2}{3})^{-\frac{1}{3}}\frac{p'Y}{\lambda(1+p')}. \tag{2.8}$$

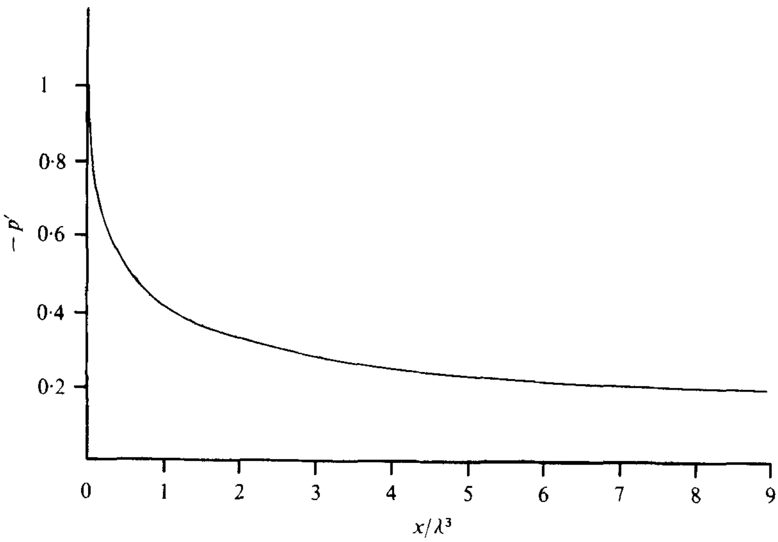

FIGURE 1. Variation in pressure gradient in slipping core region.

Here λ is an as yet arbitrary constant, f_1 and g satisfy (2.2) and (1.14*a*) with ζ_1 replaced by ξ, and

$$\lambda^3\left(\frac{1}{p'^2}-1\right)\left(\frac{1+p'}{p'}\right)p'' = -1. \tag{2.9}$$

The matching condition (2.7) requires that $f_1 \sim (\frac{2}{3})^{-\frac{1}{3}}\xi/3\lambda$ as $\xi \to \infty$, and so, from the solution of (2.2) described earlier,

$$\lambda = (\tfrac{3}{2})^{\frac{1}{3}}/3a, \tag{2.10}$$

where a is given in table 1. Integration of (2.9) yields the explicit formula

$$\frac{1}{2p'^2}+\frac{1}{p'}+\log|p'|+p' = \frac{x}{\lambda^3}-\frac{3}{2} \tag{2.11}$$

since $p' \to -1$ as $x \to 0$ from this region. As shown in figure 1, the pressure gradient decreases to zero as $x \to \infty$, with a corresponding change in the core velocity from the inlet Poiseuille flow to plug flow.

The thermal boundary layers for $x \leqslant O(\mu_0^2)$ are summarized in figure 2 to emphasize that the double layer structure is only needed for $x \ll \mu_0^2$.

2.1.3. *Fully developed region.* It is now straightforward to see that since $p' = O(x^{-\frac{1}{2}})$ as $x \to \infty$ in (2.11), and since the pressure gradient in the fully developed flow is $-\mu_0$, the renaissance of Poiseuille flow is described by writing $p' = \mu_0 P'$ in our original equation (1.7) and leaving all the other variables unaltered. This effectively leaves us with the full equations to solve, subject to the matching condition of plug flow as $x \to 0$. Although this problem is intractable analytically, it is plausible that there is a solution in which P' is $O(x^{-\frac{1}{2}})$ and T and $\psi+\frac{1}{3}y$ are exponentially small as $x \to 0$ with $(y+1)^2 \gg x$.

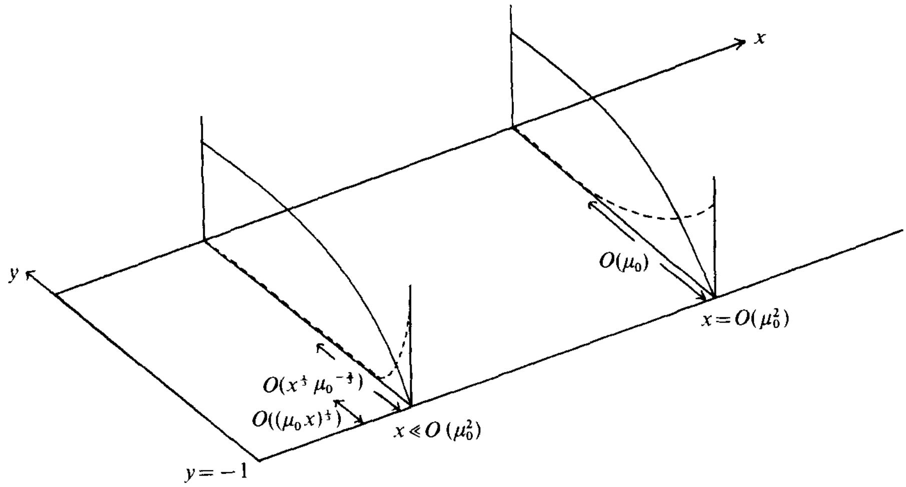

FIGURE 2. Temperature (dashed curves) and axial velocity (solid curves) variations in boundary layers in entry and slipping core regions.

2.2. *Exponential viscosity*

For simplicity we just consider $\mu = e^{-\beta T}$, although our arguments should apply whenever $\mu(\beta T) \gg \mu_0$ unless $T-1 = O(1/\beta)$.

The solution of (1.13) can no longer be analysed with the scaling (2.1) and a further subdivision becomes necessary. There is a region near the wall, denoted by a suffix 1, in which $g = 1 - g_1/\beta$ and in which $f/\zeta^2 = O(1/\mu_0)$, so that (1.13*a*) is $d^2f_1/d\zeta_1^2 = \exp(-g_1)$. Assuming $\zeta f \ll 1$, i.e. that $\zeta^3 \ll \mu_0$ in this region, we also have $d^2g/d\zeta_1^2 = 0$ to lowest order. Hence

$$g_1 \sim A\zeta_1, \tag{2.12}$$

$$f_1 \sim \frac{1}{A^2}e^{-A\zeta} - \frac{1}{A^2} + \frac{\zeta_1}{A} \tag{2.13}$$

for some constant A. There then follows a region, denoted by a suffix 2, in which g varies by $O(1)$ and in which we write $\zeta_2 = \beta^{-1}\zeta_1$, $g_2 = \beta^{-1}g_1$ and $f_2 = \beta^{-1}f_1$. Assuming

$$f\zeta = O(1) \quad \text{in region 2} \tag{2.14}$$

gives $d^2f_2/d\zeta_2^2 = \beta \exp(-\beta g_2)$, i.e. $f_2 = \zeta_2/A$ to lowest order. This in turn implies

$$\frac{d^2g_2}{d\zeta_2^2} + \frac{2}{3}\frac{\zeta_2}{A}\frac{dg_2}{d\zeta_2} = 0 \tag{2.15}$$

and any other equation for g_2 would lead to a contradiction. Now (2.14) means that $f\zeta = O(\beta^{-2})$ in region 1 and hence that, in region 1, ζ is given by

$$\zeta = O(\mu_0^{\frac{1}{3}}/\beta^{\frac{2}{3}}). \tag{2.16}$$

The region in which $\zeta = O(\mu_0^{\frac{1}{3}})$ in the algebraic case has split into two regions, one slightly thinner, in which there is an $O(\beta^{-1})$ temperature change, and one slightly thicker, in which the temperature changes by $O(1)$. We also note that (2.15) can have a solution matching with (2.12) and with $g_2 \to 1$ as $\zeta_2 \to \infty$ only if $A = (4/3\pi)^{\frac{1}{3}}$.

Finally we require an outer velocity adjustment layer as in (2.4) but where now $\zeta = O(\mu_0\beta)^{-\frac{2}{3}}, f = O(\mu_0\beta)^{-\frac{4}{3}}$ and the leading term in the expansion for f is

$$(\mu_0\beta)^{-\frac{4}{3}}[\tfrac{1}{2}\{(\mu_0\beta)^{\frac{2}{3}}\zeta\}^2 + (\tfrac{3}{4}\pi)^{\frac{1}{3}}\{(\mu_0\beta)^{\frac{2}{3}}\zeta\}]. \tag{2.17}$$

In summary, the exponential-viscosity inlet flow only differs from the algebraic case in that the temperature needs slightly more space to adjust to its core value, and this is a feature which will persist throughout the development of the flow.

From (2.17), the slipping core region now occurs when $x = O(\mu_0^2\beta^2)$ and scaling $y+1$ and $\psi+\frac{1}{3}$ by $O(\beta\mu_0)$ simply replaces (2.5) by

$$e^{-\beta T}\Psi_{YY} = -\beta\mu_0 p'. \tag{2.18}$$

For large β, (2.18), (2.6) and (2.7) are also analysed by splitting the region into one in which Y is $O(\beta^{-1})$ and T varies linearly with Y, differing from 1 by $O(1/\beta)$, followed by a region where Y and T change by $O(1)$. The similarity solution (2.8) still applies, leading to (2.9) and (2.10) with a replaced by $(\frac{3}{4}\pi)^{\frac{1}{3}}$.

There is a more dramatic contrast with the algebraic case when we consider the renaissance of the Poiseuille flow. The thermal boundary layer associated with the slipping core suggests that, when x has reached $O(1)$, the outer of the split regions, in which T varies by $O(1)$ but the shear is exponentially small, will have moved a distance $O(1)$ from the wall. Moreover the pressure gradient will have dropped only to $O(\beta\mu_0)$ rather than its fully developed value μ_0. We thus seek a solution for $x = O(1)$ in which ψ remains near $\frac{1}{3}y$ except in velocity boundary layers near the walls, and in which T adjusts to within $O(\beta^{-1})$ of 1 everywhere. Now the solution of

$$\tfrac{1}{3}T_x = T_{yy} \tag{2.19}$$

with

$$T = \begin{cases} 0 & \text{when} \quad x = 0, \quad y \neq \pm 1, & (2.20a) \\ 1 & \text{when} \quad y = \pm 1, \quad x \neq 0 & (2.20b) \end{cases}$$

gives

$$T \sim 1 - (4/\pi)\exp(-\tfrac{3}{4}\pi^2 x)\cos(\tfrac{1}{2}\pi y) \tag{2.21}$$

as $x \to \infty$. Furthermore, the velocity boundary layer in which $\psi+\frac{1}{3}$, $T-1$ and $y+1$ are $O(1/\beta)$ is described by

$$T_{YY} = 0, \quad e^{-\beta(T-1)}\Psi_{YY} = -p'/\mu_0\beta. \tag{2.22}$$

Hence

$$T = 1 - \frac{B(x)Y}{\beta}, \quad \Psi = -\frac{p'}{\beta\mu_0}\left(\frac{e^{-BY}}{B^2} - \frac{1}{B^2} + \frac{Y}{B}\right), \tag{2.23}$$

where matching with the core yields

$$-p'/(\beta\mu_0 B(x)) = \tfrac{1}{3}, \quad B(x) = 2\exp(-\tfrac{3}{4}\pi^2 x). \tag{2.24a, b}$$

Thus, by the time x has reached $(4/3\pi^2)\log\beta$, p' will have fallen to $O(\mu_0)$ and $T-1$ will be $O(1/\beta)$ everywhere. The flow will thus be able to readjust finally to its fully developed Poiseuille profile over values of x within $O(1)$ of $(4/3\pi^2)\log\beta$, and this adjustment will again be described by effectively the full equations together with the condition that T matches with (2.21) and $\psi \to \frac{1}{3}y$ as $x \to -\infty$.

3. Cooled channel wall

3.1. *Exponential viscosity*, $\mu = e^{-\beta T}$

In the solution of (1.7)–(1.9) and (1.10*b*), there is still a qualitative similarity between the cases of algebraically and exponentially varying viscosity, but now the latter is slightly easier to analyse. Again we begin with the solution of (1.13).

3.1.1. *Entry region.* We first note that, for $|g| < O(1/\beta)$, f will be exponentially small, so that, sufficiently near the wall, $g \sim -1 + c\zeta$ for some constant c depending on β. Now, from (1.13*b*), f will in general only change by $O(1)$ when ζ changes by $O(1)$. These two observations suggest that $c = c_0/\beta$ and hence the scaling $\zeta = \beta\zeta^{(1)}$. For $\zeta^{(1)} < c_0^{-1}$ the lowest-order solution is

$$f = 0, \quad g = -1 + c_0\zeta^{(1)}, \tag{3.1}$$

but near $\zeta^{(1)} = c_0^{-1}$ there is a transition region where we put $\zeta^{(1)} = c_0^{-1} + \chi/\beta$ and $g = G/\beta$. In these variables

$$e^{-G}\frac{d^2f}{d\chi^2} = 1, \quad \frac{d^2G}{d\chi^2} + \tfrac{2}{3}f\frac{dG}{d\chi} = 0 \tag{3.2}$$

with matching conditions

$$G \sim c_0\chi, \quad f \text{ exponentially small as } \quad \chi \to -\infty. \tag{3.3a}$$

We also hope to be able to match this region with the no-slip core:

$$G \sim 0, \quad f \sim \tfrac{1}{2}\chi^2 \quad \text{as} \quad \chi \to +\infty. \tag{3.3b}$$

Now the condition (3.3*a*) eliminates the doubly infinite number of possible solutions of (3.2) of the form $f \sim \text{constant} \times \chi + \text{constant}$ as $\chi \to -\infty$, while (3.3*b*) eliminates the singly infinite number of solutions in which $g \sim$ constant as $\chi \to +\infty$. We thus conjecture that (3.2) and (3.3) determine a unique value of c_0 and a unique solution for f and G apart from an unknown shift in χ. Indeed, numerical integration between $\chi = -5$ and $\chi = +5$ suggests that $c_0 \simeq 0{\cdot}986$.

Thus the thermal boundary layer at the inlet consists of a relatively thick region over which the temperature almost adjusts to its free-stream value, but where the velocity is exponentially small, followed by a thin region of thickness $O(x^{\frac{1}{3}})$ at a distance $O(\beta x^{\frac{1}{3}})$ from the wall in which the velocity adjustment takes place. This suggests that when $x = O(\beta^{-3})$ we should look for a 'free layer' of width $O(\beta^{-1})$ near $y = \eta(x) = O(1)$ such that the velocity remains exponentially small for $-1 < y < \eta$.

3.1.2. *Free layer.* For $x = O(\beta^{-3})$ the argument leading to (3.1) but now applied to the full equations (1.7) and (1.8) shows that $\psi + \frac{1}{3}$ is exponentially small and $T = -1 + (y+1)/(\eta+1)$ to lowest order when $y < \eta$. Also, in $0 \geqslant y > \eta$, away from the free layer, we expect T to be exponentially small, so that

$$\psi = \tfrac{1}{6}p'y^3 + q(x)\,y. \tag{3.4}$$

If we were to assume that the free layer could support a tangential velocity discontinuity, we should not be able to match (3.4) with the entry region as $x \to 0$. We therefore apply the condition $\psi + \frac{1}{3} = \psi_y = 0$ at $y = \eta$ to (3.4) to give

$$p'\eta^3 = 1. \tag{3.5}$$

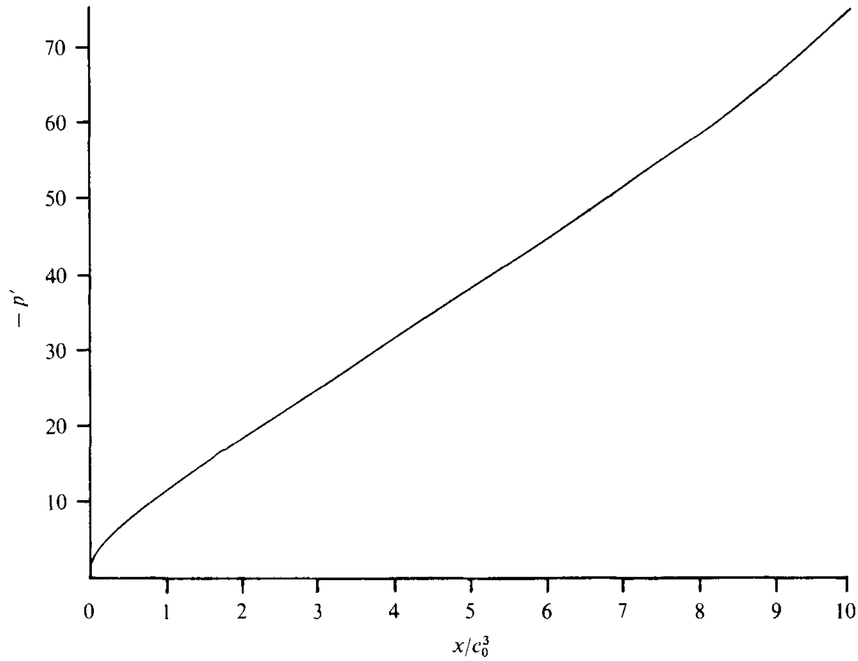

FIGURE 3. Variation in pressure gradient in free-layer region.

We can even determine p' explicitly by considering the free-layer structure. We note that if we scale $y-\eta$ and T with $O(1/\beta)$ and $\psi+\frac{1}{3}$ with $O(1/\beta^2)$, remembering that $x = O(1/\beta^3)$, we obtain

$$e^{-T}\psi_{YY} = \eta p' \tag{3.6}$$

together with (2.6) to lowest order, with matching conditions

$$T \sim Y/(\eta+1), \quad \psi \text{ exponentially small as } \quad Y \to -\infty, \tag{3.7a}$$

$$T \text{ exponentially small}, \quad \psi \sim \tfrac{1}{2}p'\eta Y^2 \quad \text{as} \quad Y \to +\infty. \tag{3.7b}$$

This system admits the similarity solution

$$T = G(\chi), \quad \Psi = h(x)f(\chi), \quad \text{where now} \quad \chi = Y/c_0(\eta+1)$$

and G and f satisfy (3.2) as long as

$$h = c_0^2\eta(1+\eta)^2 p', \quad dh/dx = 2/3c_0(\eta+1). \tag{3.8}$$

Finally, integrating (3.5) and (3.8) using $p' \to -1$ as $x \to 0$ yields

$$x/c_0^3 = \log|p'| + \tfrac{3}{2}p'^{\frac{2}{3}} + 6p'^{\frac{1}{3}} + \tfrac{9}{2} \tag{3.9}$$

(figure 3).

We note that as $x \to +\infty$ in this region

$$p' \sim -(\tfrac{2}{3}x/c_0^3)^{\frac{3}{2}} \tag{3.10}$$

and that the free layers approach within $O(\beta^{-1})$ of each other at a distance $x = O(\beta^2)$ on the free-layer scaling. By this time, p' has grown to only $O(\beta^3)$, which is much less than its fully developed value e^{β}. The variations in the thermal boundary layers before they merge are shown in figure 4.

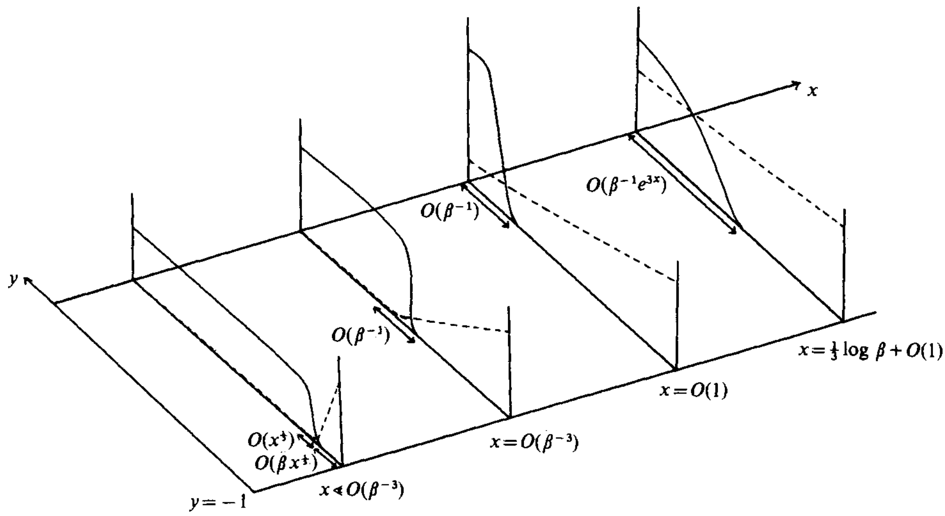

FIGURE 4. Negative temperature (dashed curves) and axial velocity (solid curves) variations in boundary layers in entry, free-layer and hot-jet regions.

3.1.3. *Hot-jet region.* The merging of the free layers is described by the full equations (1.7) and (1.8) (with $\beta = 1$); these are obtained by scaling x, y and T in the merging region with β^{-1}, and p' with β^3. In the outer region $1 \geqslant |y| > O(1/\beta)$,

$$\psi + \tfrac{1}{3} = T - y = 0 \tag{3.11}$$

to lowest order.

The situation when $x = O(1)$ is more interesting and moreover capable of explicit analysis. The merging region continues as a relatively hot jet, but one in which T varies axially by $O(1)$. Between the jet and the wall we now have

$$\psi + \tfrac{1}{3} = T - y - T_0(x)(y+1) = 0 \tag{3.12}$$

to lowest order, where $T_0(0) = 0$ to match with (3.11). However, in the jet we write

$$T = T_0(x) + T^*/\beta, \quad p' = \exp\{-\beta T_0(x)\}\beta^3 p^{*\prime}(x)$$

and scale y with $O(\beta^{-1})$, leaving x and ψ of order 1, to obtain

$$\exp(-T^*)\Psi_{YY} = Yp^{*\prime}, \quad (dT_0/dx)\Psi_Y = T^*_{YY}. \tag{3.13a, b}$$

The boundary conditions are

$$T^*_Y = \Psi = 0 \quad \text{on} \quad Y = 0 \tag{3.14a}$$

and, from matching with (3.11),

$$\Psi \sim -\tfrac{1}{3}, \quad T^* \to (1+T_0)Y \quad \text{as} \quad Y \to -\infty. \tag{3.14b}$$

Hence, from (3.13b) and (3.14b)

$$(dT_0/dx)(\Psi + \tfrac{1}{3}) = T^*_Y - T_0 - 1, \tag{3.15}$$

and so, from (3.14a),

$$\tfrac{1}{3}dT_0/dx = -T_0 - 1, \quad \text{i.e.} \quad T_0 = e^{-3x} - 1. \tag{3.16}$$

We finally conjecture that this hot-jet region persists until $T+1$ is $O(\beta^{-1})$ throughout the flow, i.e. until x is near $\frac{1}{3}\log\beta$. If we anticipate that the asymptotic solution of (3.13) and (3.14) is such that $p^{*\prime} = O(e^{-9x})$, the order of magnitude of the pressure gradient will have increased to its fully developed value when $x - \frac{1}{3}\log\beta = O(1)$, and within such a region the full equations will have to be solved in the variables ψ and $\beta(T+1)$. That this is indeed the correct additive scaling for x can be made more plausible by putting $e^{-3x} = z$ in (3.13) to give $\exp(-T^*)T^*_{YYY} = -3Yzp^{*\prime}$ with $T^*_Y = 0$ on $Y = 0$ and $T^* \sim Yz$ as $Y \to -\infty$. Now this system is invariant under the scaling $z \to \epsilon z$, $Y \to \epsilon^{-1} Y$ just as long as $p^{*\prime} \propto z^3 = e^{-9x}$. This suggests that the region in which the temperature differs from $T_0(x)$ by $O(\beta^{-1})$ is at a distance $O(1)$ from the centre of the channel when $z = O(1/\beta)$. This corresponds to putting $x - \frac{1}{3}\log\beta = O(1)$ in our original hot-jet variables.

The overall features of the merging and hot-jet regions are shown in figure 4.

3.2. *Algebraic viscosity*

We restrict attention to the case $\mu = 1 - \beta T$. The entry region is still susceptible to the scaling (2.1), in which variables (2.2a) becomes

$$-g\, d^2f_1/d\zeta_1^2 = 1 \tag{3.17}$$

to lowest order. We conjecture that there is no solution of (3.17) and (2.2b) for which $g \to 0$ as $\zeta_1 \to \infty$ but that instead there is a finite value of ζ_1, say ζ_c, in the neighbourhood of which $g \sim \frac{1}{6}(\zeta_1 - \zeta_c)^3$ and $f_1 \sim -3/(\zeta_1 - \zeta_c)$. A linearization near such a point $\zeta_1 = \zeta_c$ shows that f_1 differs from $-3/(\zeta_1 - \zeta_c)$ by $O(|\zeta_1 - \zeta_c|^\alpha)$, where α satisfies a quartic equation. This equation has two complex roots with real parts greater than 3 and two real roots less than -1. We thus expect that the three conditions (1.14b) at $\zeta_1 = 0$ will determine ζ_c uniquely. In fact, integrating (3.17) and (2.2b) numerically for different values of $g'(0)$ decreasing from $+\infty$ towards 0·569 shows that g vanishes at some value ζ_1^* which increases towards 2·65. Moreover, $g'(\zeta_1^*)$ is positive but decreases to zero as $g'(0) \downarrow 0{\cdot}569$. For $g'(0) < 0{\cdot}569$, $g < 0$ for all ζ and g tends monotonically to a negative constant as $\zeta_1 \to \infty$. We thus conjecture that ζ_c is near 2·65. The velocity will adjust to match with the core in a region in which $\zeta_1 - \zeta_c = \beta^{-\frac{1}{3}}\chi$, $g = O(\beta^{-1})$ and $f_1 = O(\beta^{\frac{1}{3}})$, where $\chi = O(1)$. In variables scaled this way, the region is described by the solution of $(1-g)\,d^2f/d\chi^2 = 1$ and $d^2g/d\chi^2 + \frac{2}{3}f\,dg/d\chi = 0$ with matching conditions $g \sim \frac{1}{6}\chi^3$ and $f \sim -3\chi^{-1}$ as $\chi \to -\infty$ and $g \sim 0$ and $f \sim \frac{1}{2}\chi^2$ as $\chi \to +\infty$. Plausibility arguments similar to those following (3.2) and (3.3) can be given for the uniqueness of the solution of this system, whose numerical solution is given in figure 5.

The layer near $\zeta_1 = \zeta_c$ again generates a free layer downstream. However it is now of thickness $O(\beta^{-\frac{1}{3}})$ and exists over a region $x = O(\beta^{-1})$ and, unlike the case of exponential viscosity, T and $\beta(\psi + \frac{1}{3})$ satisfy effectively the full coupled equations in $-1 \leqslant y \leqslant \eta$. As in the entry region, the solution in $-1 \leqslant y < \eta$ appears to determine the position of the free layer, whereas, with exponential viscosity, the structure of the free layer determined its position. The core flow in $\eta < y \leqslant 0$ is still given by (3.4), so that (3.5) remains valid, but we have found no analogue of (3.9).

The lack of an explicit solution in $-1 \leqslant y < \eta$ makes it impossible to determine the similarity variable for the free-layer region and this makes the region in which the layers merge more elusive. One possibility is that merging takes place over x and y distances $O(\beta^{-\frac{1}{2}})$, with the temperature being $O(\beta^{-1})$ and the pressure gradient $O(\beta^{-\frac{3}{2}})$. Between this merging region and the wall, ψ is still near $-\frac{1}{3}$ but T is $O(1)$. If this is the structure when $x = O(\beta^{-\frac{1}{2}})$ there will presumably then be a final region with $x = O(1)$ and $p' = O(\beta)$ within which T and ψ attain their fully developed values.

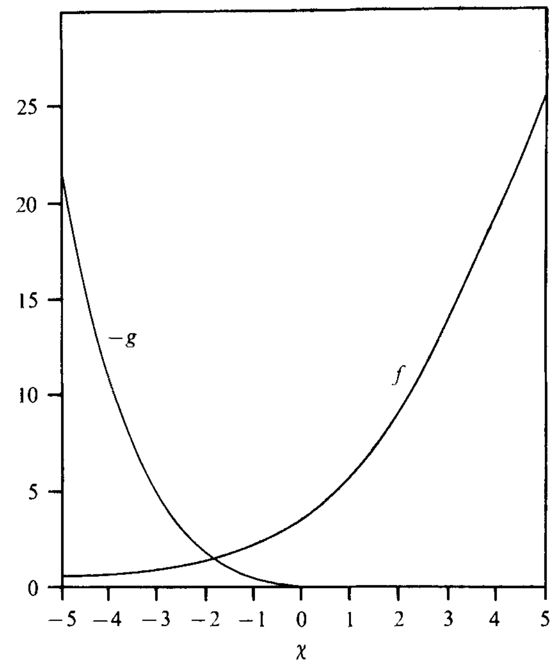

FIGURE 5. Numerical solution of

$$(1-g)\frac{d^2f}{d\chi^2} = 1, \quad \frac{d^2g}{d\chi^2}+\tfrac{2}{3}f\frac{dg}{d\chi} = 0.$$

4. Conclusion

The asymptotic techniques described above permit a qualitative and in some cases a quantitative discussion of the important features of the flow fields for a variety of viscosity/temperature laws providing only that they are sufficiently sensitive. In particular, the regions where the velocity and temperature gradients are most severe can be read off at once, as well as the relevant orders of magnitude.

As described briefly in the appendix, the methods can easily be applied to axisymmetric flow. The two most obvious differences which we have noticed are that in the cooled-wall case (3.5) is replaced by $p'\eta^4 = -1$ and that, when the viscosity is exponential, the thickness of free layer decreases downstream. This decrease is so rapid that, when the free layer nears the centre-line of the pipe, the temperature has fallen to within $O(1/\beta)$ of -1 everywhere and consequently there is no hot-jet region at all.

We should like to express our thanks to Professor S. F. Shen and Dr C. A. Hieber of Cornell University for drawing our attention to this problem and for their useful suggestions, to Dr A. B. Tayler for pointing out the basic similarity solution (1.7), and to Dr D. F. Mayers and Mr R. Branton for numerical assistance.

Appendix. Axisymmetric flow

The dimensionless equations corresponding to (1.7)–(1.10) are

$$\mu(\beta T)(r^{-1}\psi_r)_r = \tfrac{1}{2}rp', \tag{A 1}$$

$$\psi_r T_x - \psi_x T_r = (rT_r)_r, \tag{A 2}$$

where r is distance from the axis and the axial velocity is $r^{-1}\psi_r$, with

$$T = 0, \quad \psi = \tfrac{1}{8}r^2 - \tfrac{1}{16}r^4 \quad \text{at} \quad x = 0 \tag{A 3}$$

and

$$T \mp 1 = \psi_r = \psi_x = 0 \quad \text{at} \quad r = 1. \tag{A 4a, b}$$

When x is sufficiently small for p' to be near -1, we now write

$$\psi = \tfrac{1}{16} - x^{\frac{2}{3}}f(\zeta), \quad T = g(\zeta), \quad \zeta = (1-r)/x^{\frac{1}{3}}$$

to obtain

$$\mu(\beta g)\frac{d^2f}{d\zeta^2} = \tfrac{1}{2}, \quad \frac{d^2g}{d\zeta^2} + \tfrac{2}{3}f\frac{dg}{d\zeta} = 0 \tag{A 5a, b}$$

instead of (1.13).

When the wall is heated, this boundary-layer structure breaks down in the case of algebraic viscosity, as in §2.1.2, when $x = O(\mu_0^3)$. The subsequent slipping core region is described by the scalings which led to (2.5) and (2.6). Although (2.11) is still valid, the appearance of the $\frac{1}{2}$ in (A 1) and the replacement of (2.7) by $\Psi \sim \frac{1}{8}(1+p')Y$ means that (2.10) becomes

$$\lambda = 6^{\frac{1}{3}}/8a. \tag{A 6}$$

Again the full equations describe the flow downstream of the slipping core region. For an exponential viscosity, the only other slight contrast with the two-dimensional flow is that when $x = O(1)$ the plug flow is $\psi = \frac{1}{16}r^2$, with the temperature consequently being governed by $\frac{1}{8}rT_x = (rT_r)_r$. The relevant asymptotic solution as $x \to \infty$ is

$$T \sim 1 - \frac{2\int_0^1 rJ_0(\gamma_1 r)\,dr}{[J_1(\gamma_1)]^2}\exp(-4\gamma_1 x)J_0(\gamma_1 r),$$

where γ_1 is the smallest zero of $J_0(r)$, and the final adjustment to fully developed flow takes place when $x - (4\gamma_1)^{-1}\log\beta = O(1)$.

There is more contrast with the two-dimensional case when the wall is cooled. For an exponential viscosity, a free-layer analysis for $x = O(\beta^{-3})$ gives a core $r < \zeta(x)$ in which, to lowest order,

$$T \sim 0, \quad \psi \sim (\tfrac{1}{16}r^4 - \tfrac{1}{8}\zeta^2 r^2)p'. \tag{A 7}$$

This core is separated by the free layer from a stagnant region in which

$$\psi \sim \tfrac{1}{16}, \quad T \sim -1 + \log r/\log\zeta. \tag{A 8}$$

Hence, instead of (3.5),

$$\zeta^4 p' = -1. \tag{A 9}$$

The similarity solution in the free layer is

$$T = \beta^{-1}G(\chi), \quad \psi = \tfrac{1}{16} - (2^{-\frac{8}{3}}c_0^2/\beta^2)(\log\zeta)^2 f(\chi),$$

where

$$\chi = \beta(r-\zeta)/2^{-\frac{4}{3}}c_0\zeta\log\zeta. \tag{A 10}$$

We find

$$e^{-G}\frac{d^2f}{d\chi^2} = \tfrac{1}{2}, \quad \frac{d^2G}{d\chi^2} + \tfrac{2}{3}f\frac{dG}{d\chi} = 0 \qquad \text{(A 11), (A 12)}$$

as long as

$$\zeta = \exp\{-(2x)^{\frac{1}{3}}/c_0\}, \qquad \text{(A 13)}$$

which implies

$$p' = -\exp\{4(2x)^{\frac{1}{3}}/c_0\}. \qquad \text{(A 14)}$$

The distance of the free layer from the axis is comparable with its thickness when $\zeta \sim e^{\beta}$, by which time p' has increased to the order of magnitude of its fully developed value and our unscaled x variable is $O(1)$. The free-layer region merges into a region described by the full equations, where $T+1 = O(1/\beta)$, and there is no hot jet as in the two-dimensional case. Finally, when the viscosity is algebraic, there is a free layer of width $O(\beta^{-\frac{1}{3}})$ when $x = O(\beta^{-1})$ but still no similarity solution.

REFERENCES

Craik, A. D. D. 1968 *J. Fluid Mech.* **36**, 685.

Galili, N., Takserman-Krozer, R. & Rigbi, Z. 1975 *Rheol. Acta* **14**, 550–567.

Horve, L. A. 1974 *J. Elast. Plast.* **6**, 160.

Lebon, G. & Nguyen, H. 1974 *Int. J. Heat Mass Transfer* **17**, 655.

Lord, H. A. & Williams, G. 1975 *Polymer Engng Sci.* **15**, 553, 569.

Munahata, T. 1975 *Int. Chem. Engng* **15**, 193.

Pearson, J. R. A. 1977 *J. Fluid Mech.* **83**, 191.